Numerical Analysis of Pile Behavior under Lateral Loads in Layered Elastic–Plastic Soils

Zhaohui Yang and Boris Jeremić[*]

Department of Civil and Environmental Engineering, University of California,

Davis, CA 95616

SUMMARY

This paper presents results from a finite element study on the behavior of a single pile in elastic–plastic soils. Pile behavior in uniform sand and clay soils as well as cases with sand layer in clay deposit and clay layer in sand deposit were analyzed and cross compared to investigate layering effects. Finite element results were used to generate $p - y$ curves and then compared with those obtained from methods commonly used in practice.

[*]Correspondence to: Boris Jeremić, Department of Civil and Environmental Engineering, University of California, One Shields Ave., Davis, CA 95616, `jeremic@ucdavis.edu`

1. INTRODUCTION

The $p - y$ approach (Reese et al. [12]) has been widely used to design piles subjected to lateral loading. Based on the Winkler foundation theory, the method models the lateral soil-structure interaction with empirically derived nonlinear springs. The advancement of computer technology has made it possible to study this problem using more rigorous Finite Element Method (FEM).

Mentioned are a few representative finite element applications. Maqtadir and Desai [9] studied the behavior of a pile-group using a three dimensional program with nonlinear elastic soil model. An axisymmetric model with elastic-perfectly plastic soil was used by Pressley and Poulos [11] to study group effects. Brown and Shie [2] [1] [3] and Trochanis [15] conducted a series of 3D FEM studies on the behavior of single pile and pile group with elastic-plastic soil model. In particular, interface element was used to account for pile-soil separation and slippage. Moreover, Brown and Shie derived $p - y$ curves from FEM data, which provide some comparison of the FEM results with the empirical design procedures in use. A number of model tests of free- or fixed-headed pile groups under lateral loading has been simulated by Kimura et al. [6] and Wakai et al. [16] using 3D elasto-plastic FEM. A good correlation between the experiments and the analysis has been observed in these studies. All these results demonstrated that FEM can capture the essential aspects of the nonlinear problem. It is noted that there is not much literature reporting on FEM studies of pile behavior under lateral loading in layered soil system. In addition to that, there is a very small number of studies on the effects of layering system on the commonly used $p - y$ curve approach.

This paper describes four 3D finite element models of a laterally loaded pile embedded in uniform and layered soil profiles with the dimensions and soil parameters similar to those used

in the centrifuge study by McVay et al. [8] and Zhang et al. [7]. The bending moments derived by integrating vertical stresses from FEM are numerically differentiated once and twice to compute the shear force and pressure diagrams, respectively. Particularly, $p - y$ curves are generated and cross compared to illustrate the effects of soft clay (sand) layer on the $p - y$ curves of the overlaid sand (soft clay) layer. The results from FEM are also compared with those from centrifuge test and LPILE. In addition, a limited parametric study of pressure redistribution is conducted by changing the undrained shear strength of the soft clay layer and the friction angle of the sand layer to further investigate the layering effects. The OpenSees [10] finite element framework was employed to complete all the computations. Soil modeling was performed using Template Elastic–Plastic approach (Jeremić and Yang [5]).

2. Constitutive Models

Two simple models were used in this numerical study. Specifically, clay was modeled by a simple von Mises material model which is completely defined with the undrained shear strength. Sand was simulated by a Drucker–Prager material model with non-associated flow rule. The reason for using such simple models is that the experimental results used to compare our simulations against did specify only those two material properties for sands and clays. Figure 1 presents yield surfaces for both models. In both material models, the Young's moduli vary with confining pressure, as shown in Eqn. (1).

$$E = E_o \ \left(\frac{p}{p_a} \right)^a \tag{1}$$

where E_o is Young's Modulus at atmospheric pressure, p is the effective mean normal stresses, p_a is the atmospheric pressure, and a is constant for a given void ratio. In this work, 0.5 was used.
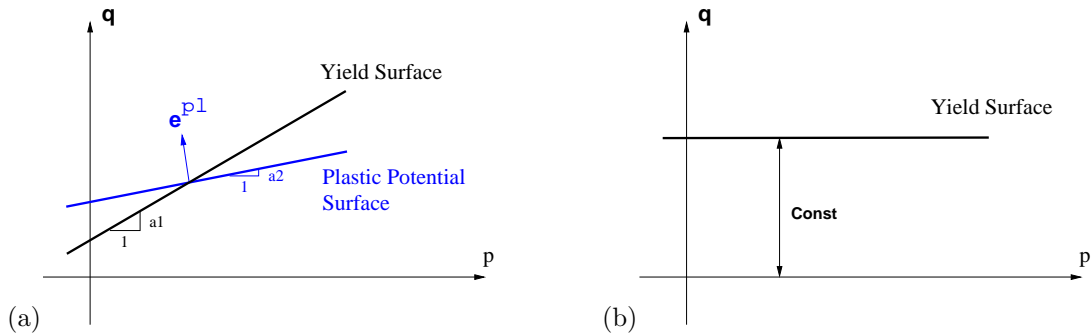
Figure 1. Elastic plastic models used in this study: (a) Drucker–Prager model specified with friction angle and dilation angle, and (b) von Mises model specified with undrained shear strength C_u.

The following parameters were used for medium dense sand: friction angle ϕ of 37.1^o, Shear modulus at a depth of 13.7 m of 8960 kPa ($E_o = 17400$ kPa), Poisson's ratio of 0.35 and unit weight of 14.50 kN/m^3. These parameters were given by Zhang et al. [7]. A dilation angle of 0° is used in this work (Brown and Shie [2]). The undrained shear strength, Young's modulus, Poisson's ratio and unit weight of clay were chosen to be 21.7 kPa, 11000 kPa, 0.45, 13.7 kN/m^3, respectively. It should be noted that the above material models are available within the OpenSees finite element platform using Template Elastic–Plastic Material Modeling paradigm (Jeremić and Yang [5]). It should also be noted that the use of simple Drucker–Prager model can over-predicted the friction angle to triaxial extension stress path. However this influence is limited to the zone behind the pile, within the interface zone and thus this drawback of the Drucker–Prager model was neglected.

3. SIMULATION RESULTS

Presented in this section are representative results related to the behavior of piles in uniform and layered soil systems. Presented results are compared with those from the centrifuge study (McVay et al. [8]), and with results obtained using LPILE program (Reese et al. [12, 13].

3.1. Pile Models

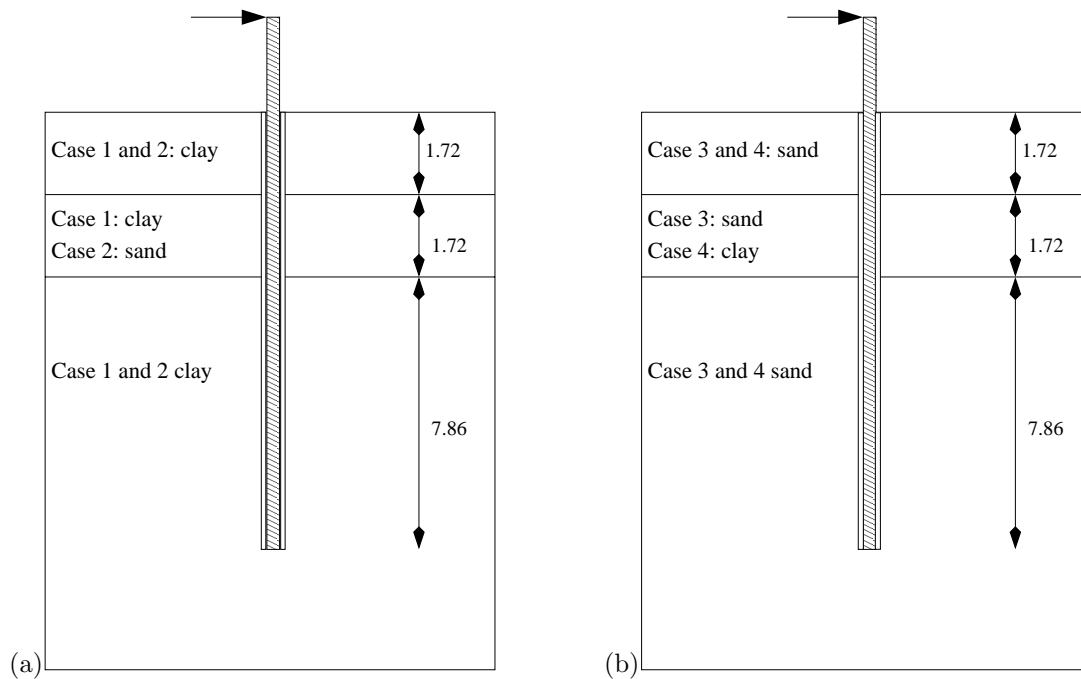A number of static pushover tests for single pile models were simulated using uniform soil and layered soil setups. Figure 2 shows the model setups. There are four main setups. Two of these

Figure 2. (a) Single pile models, dimensions and layers of case #1 and #2. (b) Single pile models, dimensions and layers of case #3 and #4.

are dealing with uniform sand and clay soils, while two others are featuring layered soils. In

particular, the case # 1 is a uniform soft clay soil, case # 2 includes top and bottom layers of soft clay with an in–between layer of medium dense sand. On the other hand, case # 3 features uniform medium dense sand soil, while case # 4 features top and bottom layers of medium dense sand with an in–between layer of soft clay. Detailed layering setup is given in Figure 2.

Figure 3 shows the finite element mesh for all four cases. Based on symmetry, only half of the model is meshed. Twenty node brick elements are used for both soil, pile and interface. It should be noted that these quadratic elements exhibit high accuracy even for high aspect ratios and can model accurately bending of solid piles with two layers of elements. During mesh design stage, a study was performed to decide on appropriate (balanced) mesh size. That study showed that a much larger mesh, with many more elements (with lower aspect ratios) would account for a fairly small change in results, so it was decided that the current mesh is sufficient for our analysis.

The square pile, with a width of 0.429 m, consist of four elements (per cross section) with the elastic property of aluminum. The fine mesh in the upper part of the model is to provide data points for the computation of shear forces and $p - y$ curves of sufficient reliability as well as for the investigation of layering effects. The sides and bottom of the model are fixed with the exception of the symmetric boundary, which is only supported in Y direction. The interface layer between aluminum pile and surrounding soil is represented by one thin layer of elements. The purpose of this layer is to mimic the installation effects on piles (drilled or driven). It also serves a purpose of a simplified interface which allows for tension cut-off (gaping) and controlled, coupled horizontal and vertical stiffness. All interface elements were simulated by Drucker–Prager model with a friction angle of 25°, and a dilation angle of 0°.
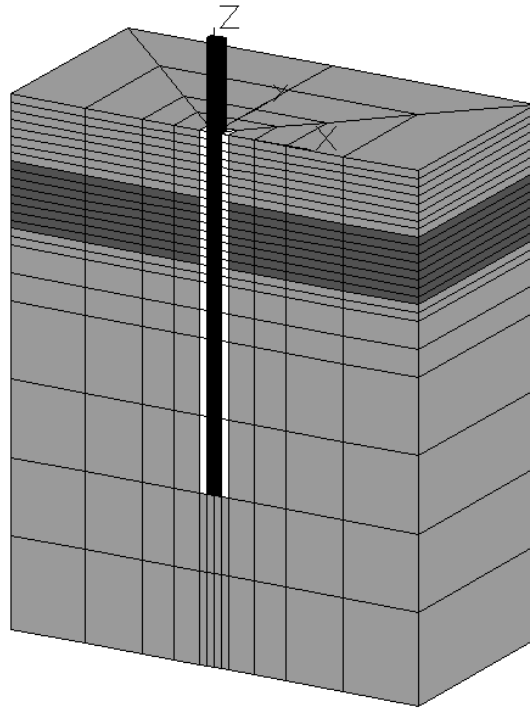
Figure 3. Mesh of single pile model, side view, top eight layers of finite elements are either clay or sand (depending on the cases), middle eight layers of finite elements are sand or clay (again depending on the cases) and the bottom is all uniform clay or sand, interface zone around the aluminum pile is also present.

3.2. Plastic Zones

The static pushover test were conducted using load control at pile head. The final plastic zones are depicted in Figures 4, 5. Plastic zones are actually presented by plastified Gauss points. In particular, Figure 4(a) shows developed plastic zones for the uniform clay soil (case # 1). It is interesting to note that the plastic zone propagates fairly deep while it does not extend far from the pile in clay. Moreover, compression side (right side) features much larger plastic zone while the plastic zone for the extension side (left side) is confined to the interface layer and

a few Gauss points outside the interface layer. The case with clay and sand layer in–between

is shown in Figure 4(b). The main difference is that the plastic zone is even smaller than for

uniform clay layer. It is worth mentioning that this case, which includes sand layer, is stiffer

than the uniform clay case, thus displacements are smaller in clay and the plastic zone does

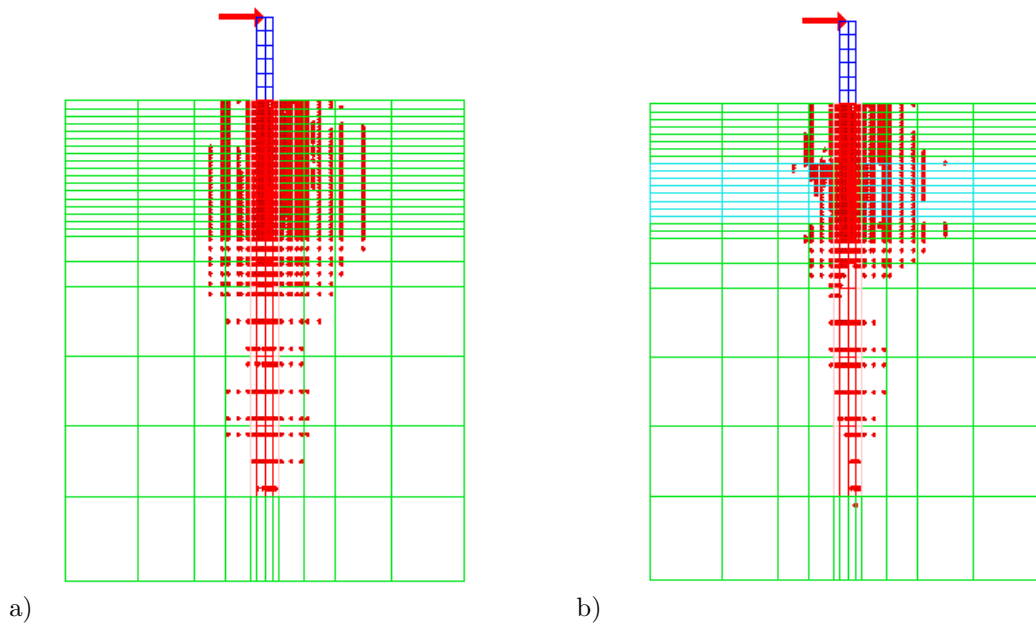not propagate as much as in uniform clay soil.

a)   b)

Figure 4. The plastic zones for (a) case # 1, and (b) case # 2 at lateral loading of 400kN.

Figure 5(a)(b) shows plastic zones at the end of loading process for sand and sand and clay

soils. In particular, Figure 5(a) shows the plastic zone for uniform sand. It is interesting to

note that the plastic zone propagates toward the surface with the collapse mechanics similar

to the active and passive failure. In this case of course the system is 3D and so the failure

propagation angles do not match the active and passive failure angles, however the difference

between active and passive zones propagation angles is almost exactly $\pi/2$. Figure 5(b) shows

plastic zone for the case # 4 which includes a layer of clay between -1.72m and -3.44m (Z

coordinate, origin is in the pile center at the ground surface) . It is noted that the plastic zone

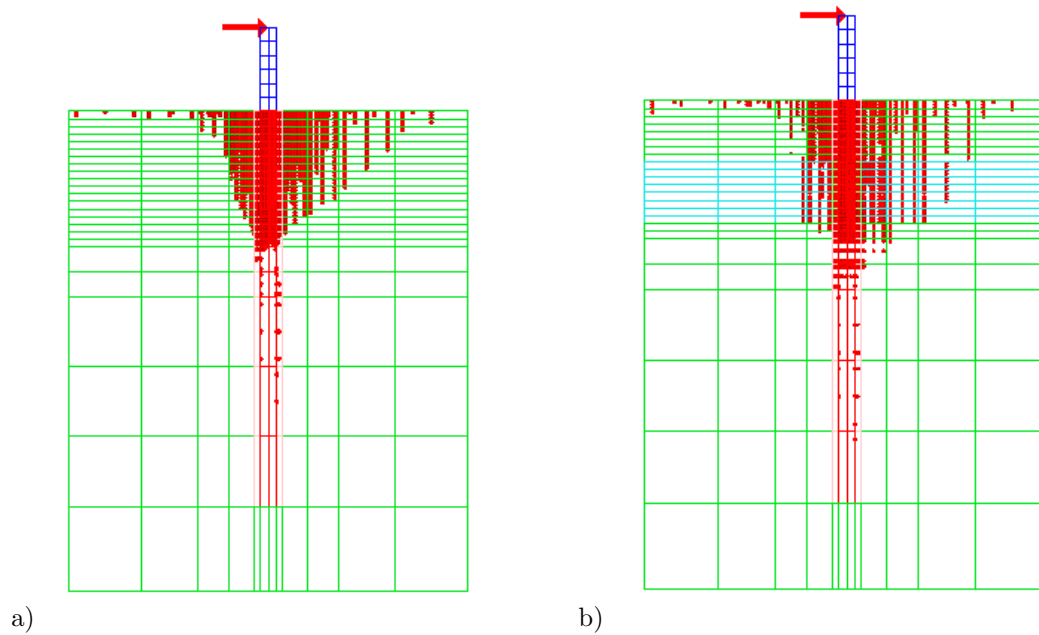is deeper, but not as nicely defined as in the previous case.

a)   b)

Figure 5. The plastic zones of case 3 and 4 at lateral loading of 400kN.

3.3. $p - y$ Curves

Results from static pushover tests on piles were used to generate $p - y$ curves. The bending

moments derived by integrating vertical stresses are numerically differentiated once and twice

to compute the shear force and pressure diagrams, respectively. Direct integration of shear

stresses was also performed to check results and it was found that shear forces were within 5%

accuracy. The combination of calculated pressures (p) and displacements obtained from the

finite element solution, allowed for generation of $p - y$ curves at various depths along the pile.

In what follows, presented are generated $p - y$ curves for both uniform soils (sand and clay) as well as for layered systems. It is noted that the graphical presentation of results for bending moments, shear forces and lateral pressures (load) on a pile beam are shown with 10 lines, each one representing results for one increment (1/10) of the total load.

Uniform Clay Soil.   Figure 6 shows bending moments, shear forces and pressures along the depth of a pile in clay soil. It should be noted that the maximum bending moment, as well as the switching of sign for shear force, moves quite a bit from the depth of approximately -1.7m all the way to the depth of -3.4m. Pressure distribution shows that the top layers are already at the ultimate values of pressures and thus the pressure diagram propagates downward. There is a slight fluctuation of pressures at the depths of $4 - 5$m, which is attributed to the small numerical problems while doing double differentiations.

Figure 7 shows generated $p - y$ curves for uniform clay layer. It is obvious that most of the clay (at least until the depth of -2.6m) has reached its peak resistance.

Uniform Sand Soil.   Figure 8 shows bending moments, shear forces and pressures for a pile in a uniform sand soil. In this case it is interesting to note that the maximum bending moment, as well as the change of sign for the shear force is moving only between the depths -1.8m and -2.0m. Moreover, the pressure diagram shows steady increase (with top layers reaching ultimate pressures) until the depth of -1.7m and then steadily decreases, and changes sign at greater depths (below -4.0m).

Figure 9 shows generated $p - y$ curves for the uniform sand case. It is interesting to note that only the top layer at the depth of about -0.3m will reach the ultimate pressure. All the
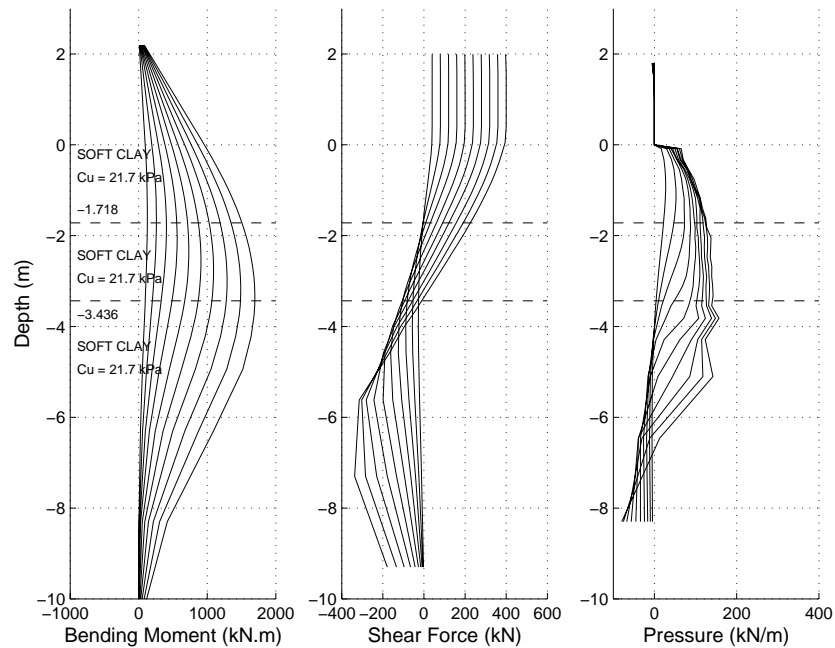
Figure 6. Bending moment, shear force and pressure distributions for the uniform clay profile.

other sand material is far away from corresponding ultimate pressures. It is also worth noting that the displacements in the case of uniform sand are much smaller (almost twice as small) than what has been observed in uniform clay case.

Clay Soil with a Layer of Sand.   Figure 10 shows bending moments, shear forces and pressures for a layered soil case. In this case a layer of sand extends from $-1.72m$ to $-3.44m$. The rest of soil is soft clay. It is interesting to note a large jump in pressures for the sand layer (as expected) and that the pressures in the top clay layer (from the surface to $-1.7m$) reaches ultimate values. Small non–uniform distribution of the pressures at the interface of sand and clay at $-3.44m$ is attributed to the coarseness of the finite element mesh. In comparing Figure 10 with the results for uniform clay case (Figure 6) it is obvious that the sand layer arrests the
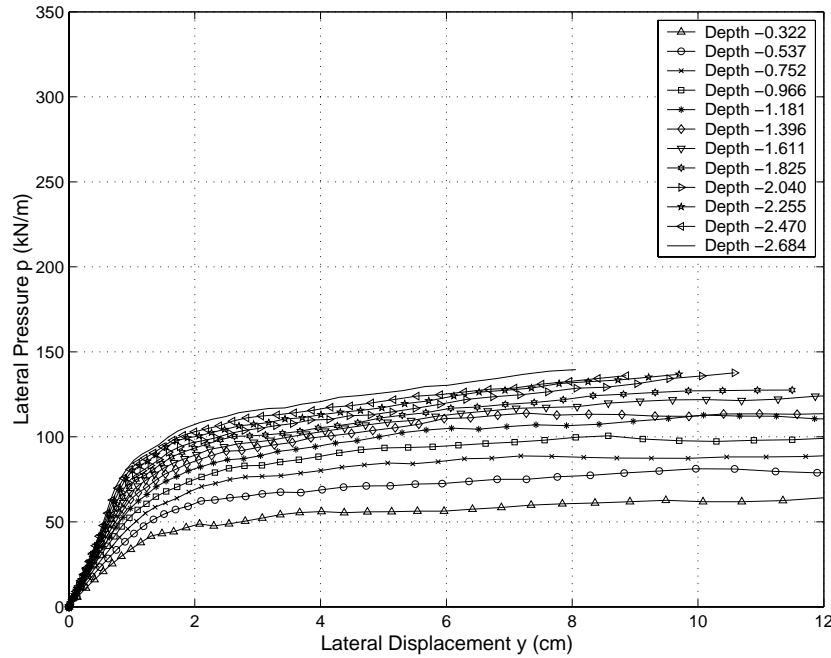
Figure 7. Calculated $p - y$ curves for the uniform clay profile.

propagation of deformation and forces in depth and fixes the maximum moment to approx. $-2.1m$.

Figure 11 shows generated $p - y$ curves for the layered case (single layer of sand in clay). The $p - y$ curves were generated only for the top layer of clay and middle layer of sand, to the depth of $-2.7m$. It is interesting to note that the $p - y$ curve for clay at the depth of $-1.61m$ (close to the sand layer) exhibits strong hardening, unlike similar curve for the uniform clay soil, in Figure 7. The increase in pressure (transversal loading on the pile) between uniform clay (Fig. 7) and clay underlain by a medium dense sand layer (Fig. 11) at the displacement of $0.06m$ is more than two times.
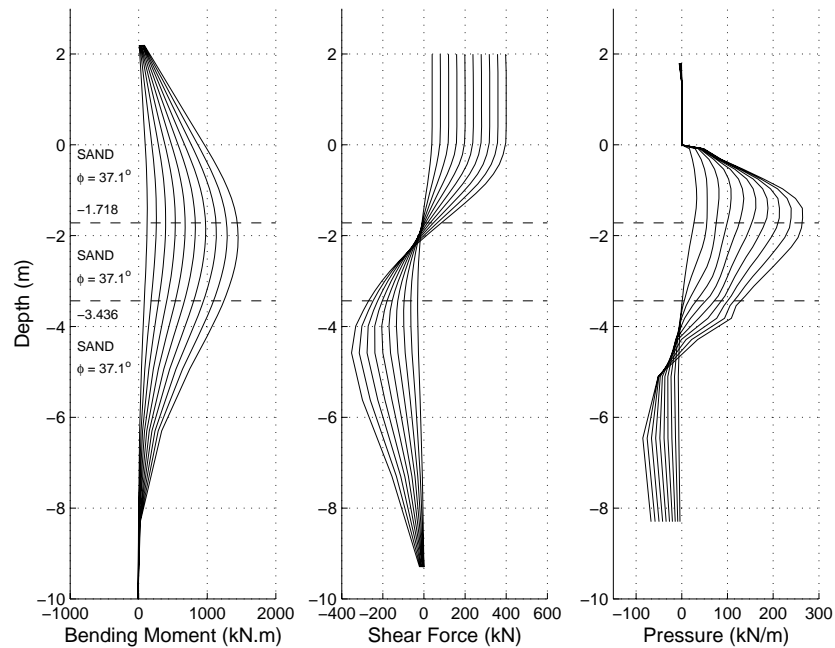
Figure 8. Bending moment, shear force and pressure distributions for the uniform sand profile.

Sand Soil with a Layer of Clay. Figure 12 shows bending moments, shear forces and transversal pressures for a case where a layer of soft clay is present within sand soil. Unlike the case of uniform sand soil (Figure 8) the presence of soft clay layer will change the depth of maximum moment by almost $1m$ (from $-2.0m$ to $-3.0m$). In addition to that, the distribution of pressures on a pile is changed significantly, as seen in the right plot of Figure 12. The reduction of pressures will extend into the sand layer and present significant influence of soft clay on pressures in sand.

Figure 13 shows generated $p-y$ curves for the case of sand with a soft clay layer. It is noted that the $p-y$ curves for sand that is some distance away from the interface with clay are much the same as for the uniform sand case (refer to Fig. 9 and Fig. 19(a)). However, the $p-y$ curves
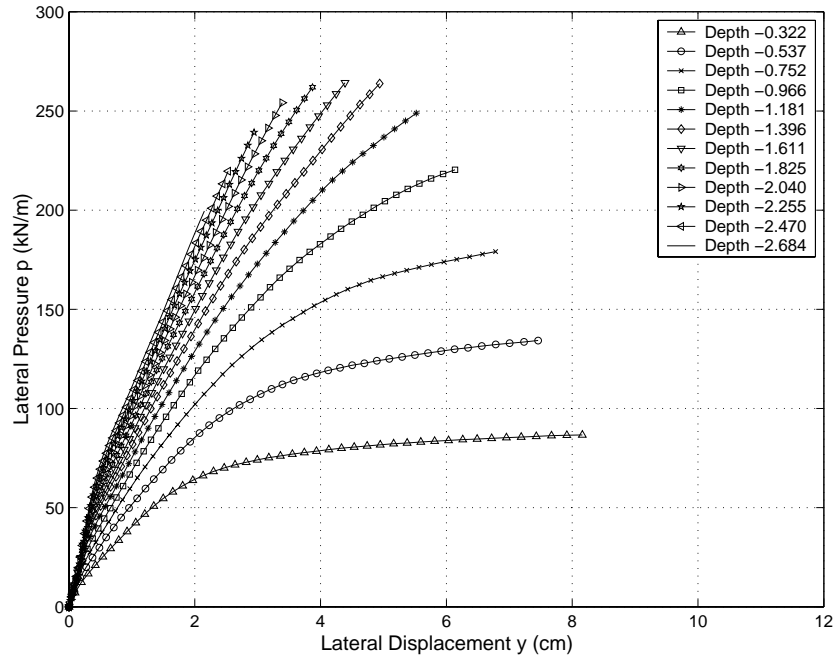
Figure 9. Calculated $p - y$ curves for the uniform sand profile.

in sand close to the interface are changed in some cases significantly. For example, the $p - y$ curve at depth of $-1.61m$ is showing pressure of approx. $p = 265kN/m$ at the displacement of $0.042m$ for the uniform sand case, while the same $p - y$ curve, still in sand, has a drop in pressure at the same displacement to $p = 140kN/m$. Similar trend is observed for other $p - y$ curves close to the interface of sand with clay.

3.4. Comparisons of Pile Behavior in Uniform and Layered Soils

Comparison of pile behavior in uniform and layered soils can also be performed by looking at the displacement and bending moment distributions. For example, Figure 14 compares the distributions of displacements for the uniform sand case with the sand and clay layer case. First
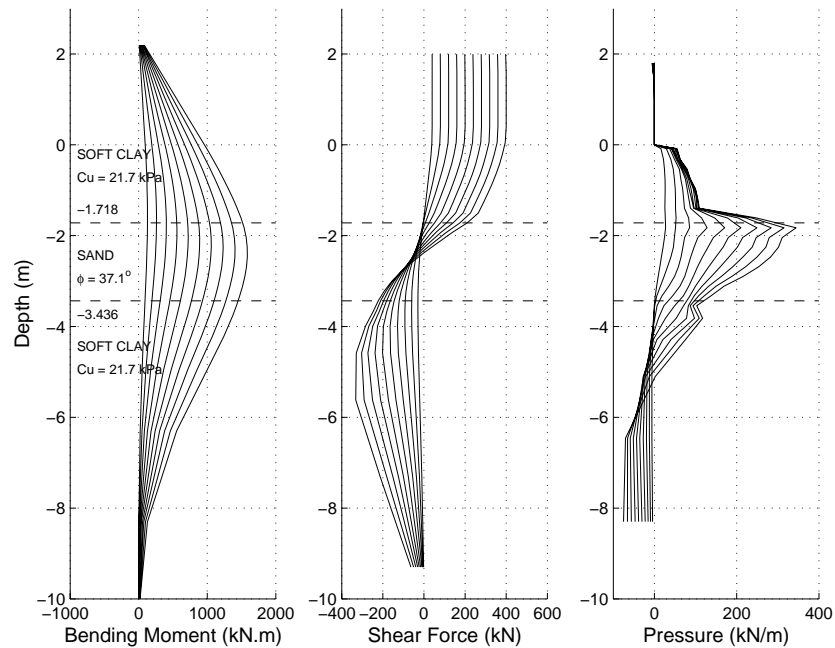
Figure 10. Bending moment, shear force and pressure distributions for the clay soil with a sand layer.

observation is that the uniform sand layer allows smaller displacements of the pile head $(0.12m)$ while the inclusion of clay layer raises those displacements to $0.22m$. Second observation is that the point of rotation for the pile (point which does not move as the loading is applied) is pushed deeper, from $5m$ to approximately $6m$. Moreover, the propagation of displacements along the depth of a pile is much greater for a layered case, the surface displacement is extended from $0.09m$ to almost $0.13m$.

Figure 15 shows similar results for uniform clay and clay with a layer of sand case. In this case, the inclusion of a sand layer will increase the stiffness of the pile (as expected) and will also reduce propagation of displacements with depth.

Figure 16 shows comparison of pile head displacements for all four cases. It is noted that
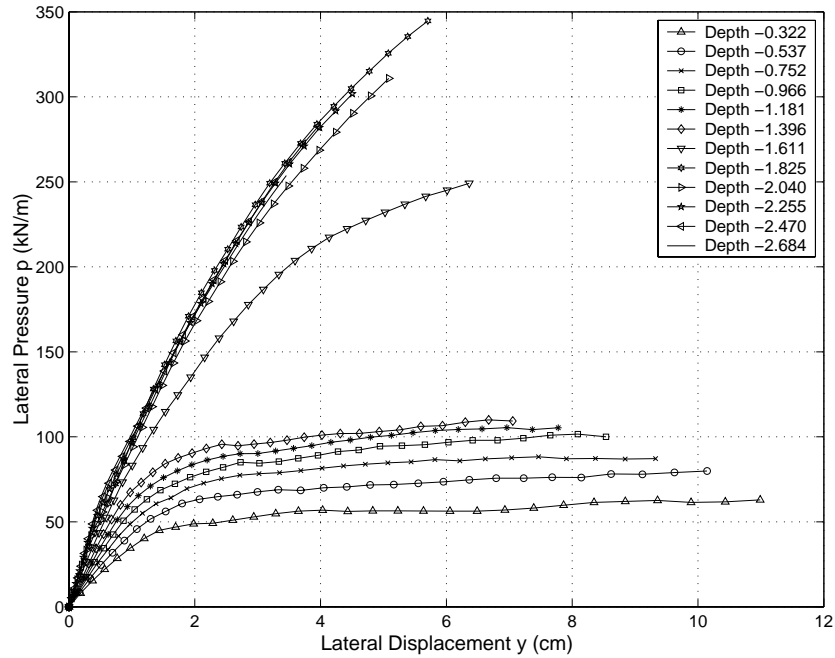
Figure 11. Calculated $p - y$ curves for the clay soil underlain by a medium dense sand layer.

the two layered cases exhibit similar behavior in terms of displacements, both at the pile head
and in terms of displacement profiles (compare right plot in Fig. 14 and left plot in Fig. 15).

Figure 17 shows comparison of the maximum bending moment calculated for the pile for
all four cases. It is interesting to note that the difference between the two uniform soil cases
(uniform sand and uniform clay) is not that pronounced. Of course one has to remember that
the material for pile was assumed to be linear elastic, no yielding was allowed for the aluminum
pile.

The $p - y$ curves for uniform clay and clay with a layer of sand were plotted together in
Figure 18 (a) for comparison. It can be seen that all the $p - y$ curves in clay except the one
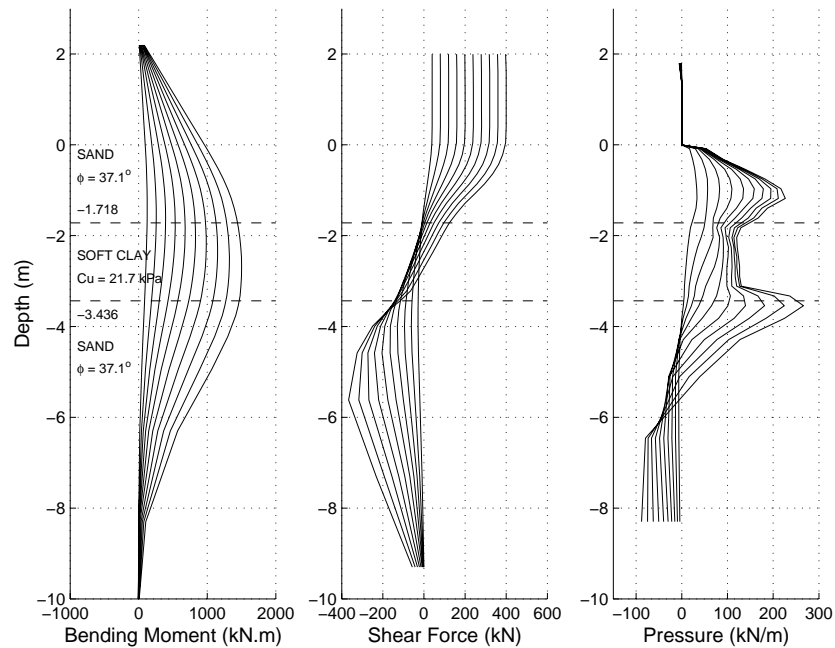right next to the layer interface are almost identical. In order to measure the magnitude of

Figure 12. Bending moment, shear force and pressure distributions for the sand soil with a soft clay layer.

the effects of sand layer on the pressure of soft clay layer, the ratio of pressures in clay layer for clay soils with a sand layer and uniform clay soils lateral displacement of 12%D, i.e. 5.15 cm, were computed and plotted against the distance in terms of times of pile width D in Figure 18. It is noted that the disturbance to the pressure field is much more confined to the immediate vicinity (within 0.75D) of the layer interface. In addition, the results from two more analysis of the same model with different sands (friction angles $\phi' = 25^o, 30^o$ respectively, other parameters remain the same.) were included in Figure 18. It is shown that the lateral pressure ratio is affected considerably when sand friction angle increases from 25° to 37° (from 1.5 times to 2.2 times more pressure).

The $p - y$ curves for uniform sand and sand with a layer of soft clay were also plotted

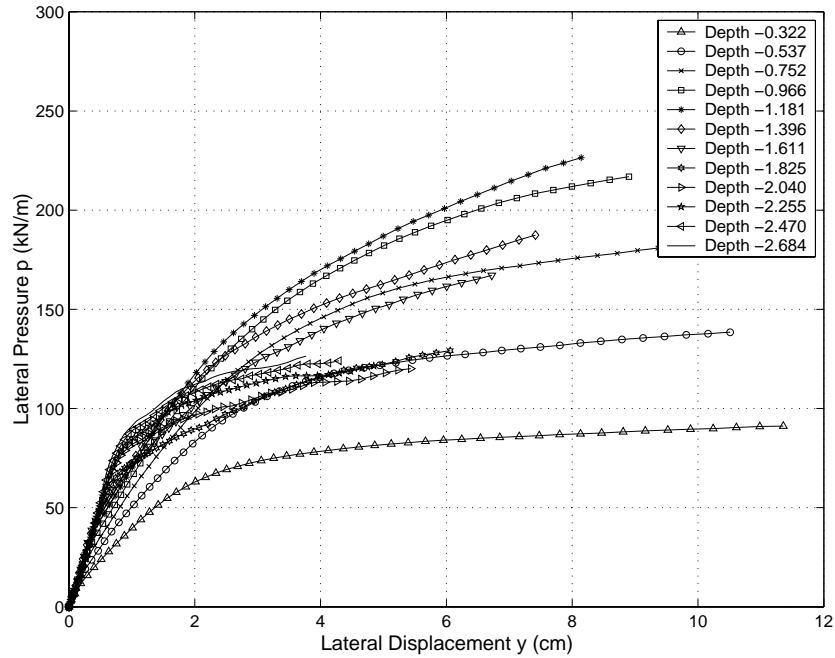*Int. J. Numer. Anal. Meth. Geomech.* 2002; **02**:1–31

Figure 13. Calculated $p - y$ curves for the sand soil underlain by a soft clay layer.

together for comparison purposes. It was found that the effect of soft clay on the pressures in sand propagates far away from the layer interface. Therefore, three cases of an additional model with a thicker sand layer (2.4m in thickness) underlain by a soft clay layer were analyzed by varying the undrained shear strength ($C_u = 13.0\ kPa,\ 21.7\ kPa,\ 30.3\ kPa$) of the soft clay layer. Similarly, the pressure ratios at 6.5% D, i.e. 2.8 cm, were plotted in Figure 19. It is noted that the effects extends to as far as 4.75D from the layer interface and the reduction of pressures adjacent to the interface is about 0.6 in all three cases.

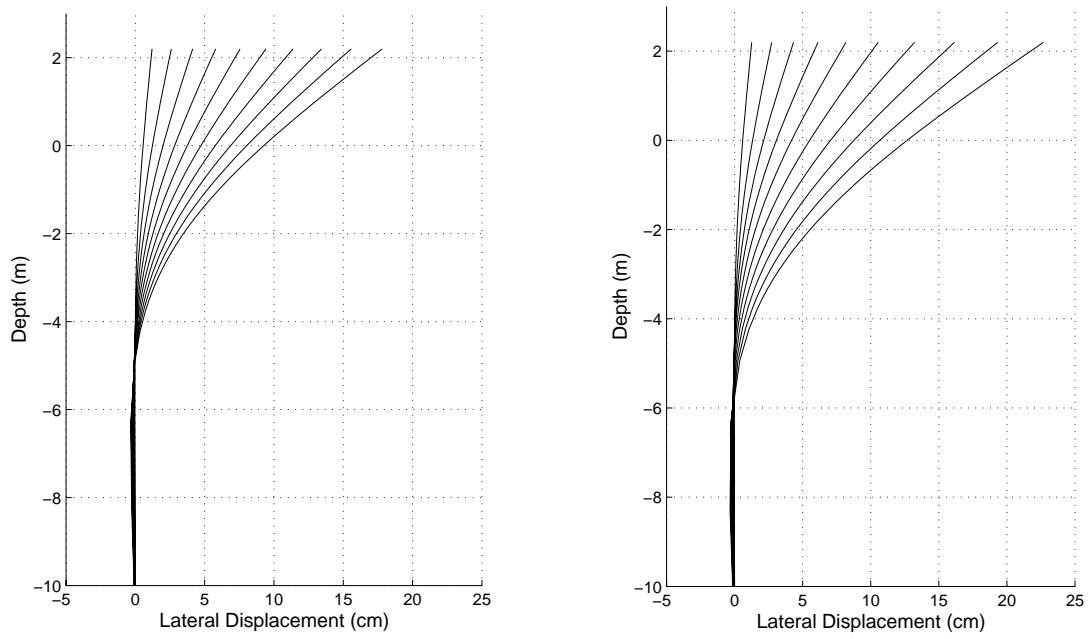*Int. J. Numer. Anal. Meth. Geomech.* 2002; **02**:1–31

Figure 14. Pile displacement distributions along the depth in a uniform sand profile (left) and sand with clay layer profile (right).
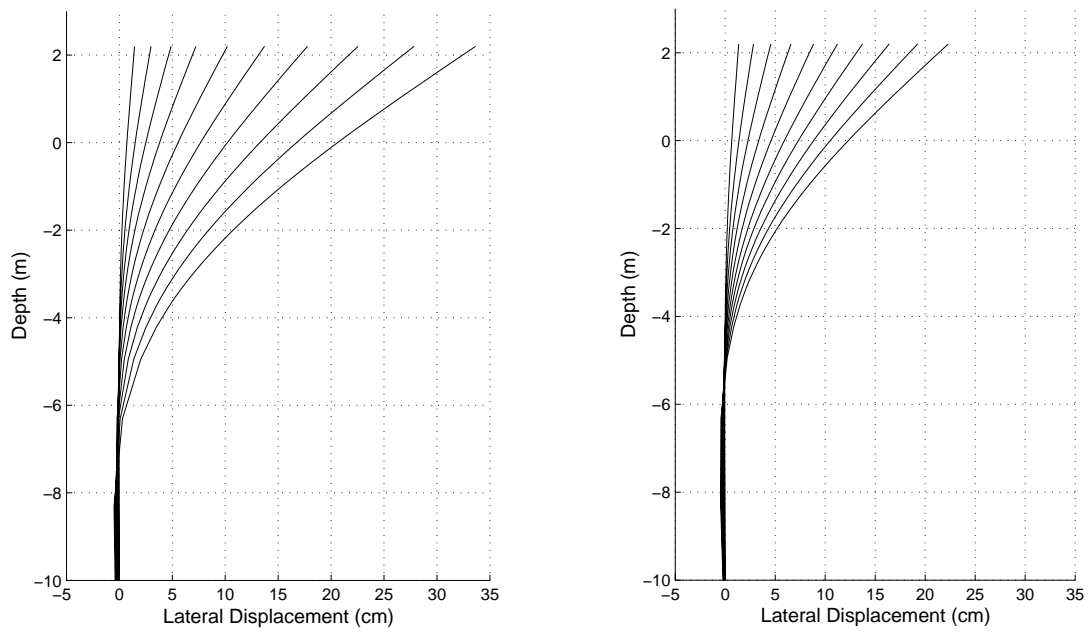
Figure 15. Pile displacement distributions along the depth in a uniform clay profile (left) and clay with sand layer profile (right).
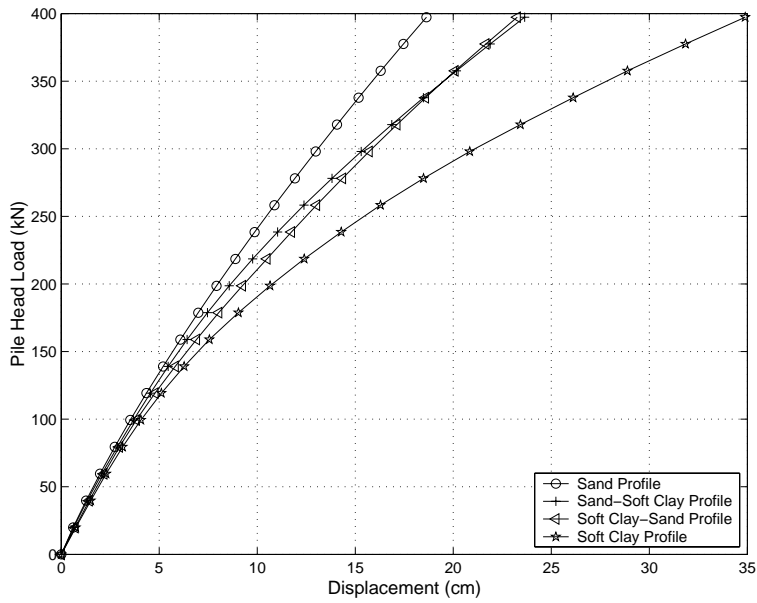
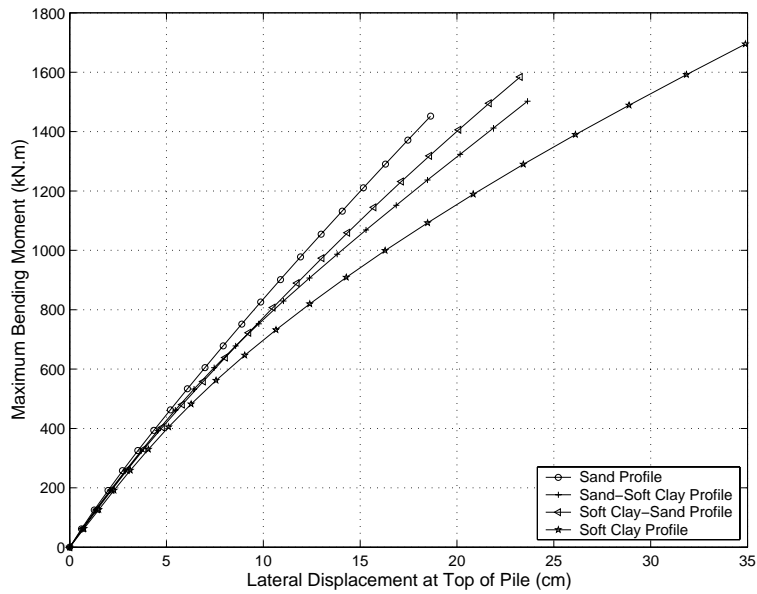Figure 16. Pile head displacement comparison for all the four cases.

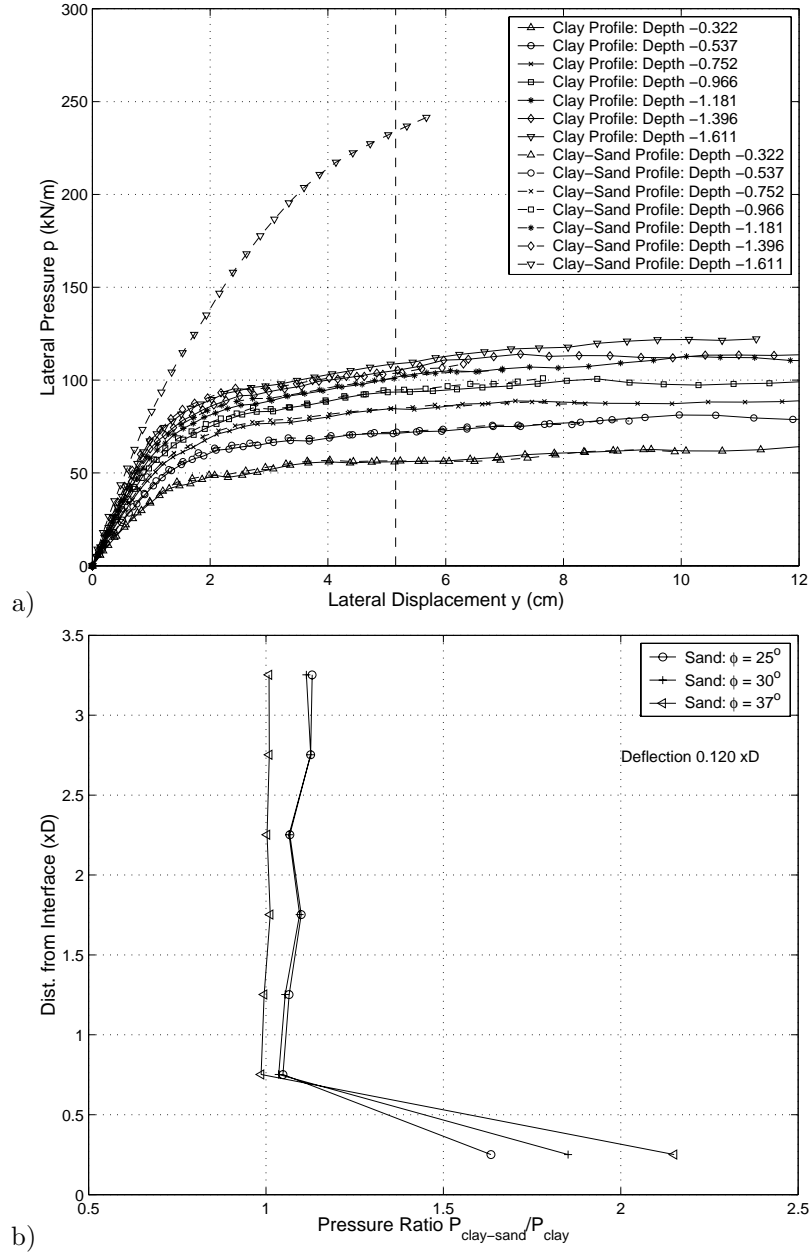Figure 17. Maximum bending moment comparison for all the four cases.

Figure 18. (a) Comparison of $p-y$ curves for uniform clay versus clay with a layer of sand ($\phi' = 37^o$).

(b) Pressure ratio distributions in clay layer for sands with different friction angle ($\phi' = 25^o$, 30°, 37°).
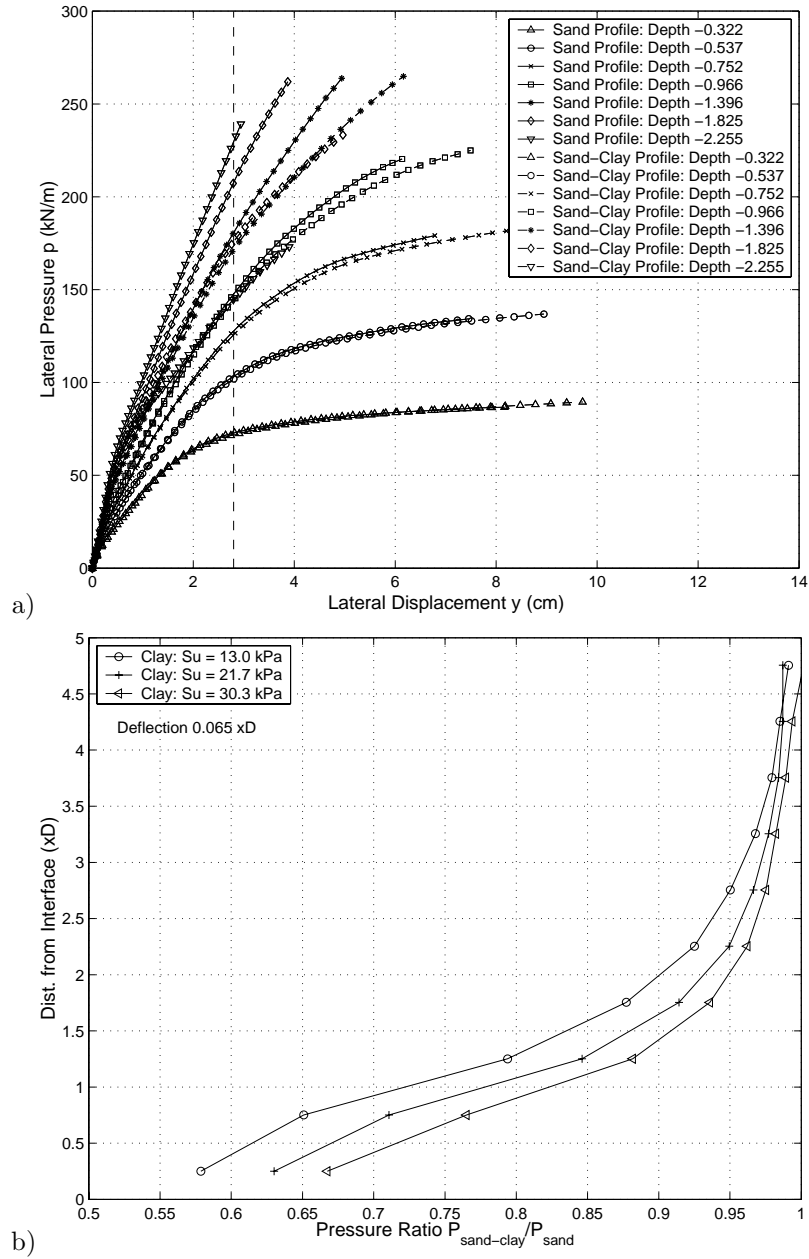
a)

b)

Figure 19. (a) Comparison of $p - y$ curves for uniform sand versus sand with a layer of soft clay ($C_u = 21.7\ kPa$). (b) Pressure ratio distributions in sand layer for clays with different undrained shear strength ($C_u = 13.0\ kPa,\ 21.7\ kPa,\ 30.3\ kPa$).

Prepared using **nagauth.cls**

3.5. Comparison to Centrifuge Tests and LPile Results

The pile head displacements for uniform sand profile from 3D FEM, LPILE (Reese et al. [12, 13]), and centrifuge test (McVay et al. [8]) were plotted against pile head load in Figure 20. It can be seen that they agree with each other fairly well. It should be noted that the material properties for our 3D finite element simulations were not in any particular way calibrated to improve the results. They were simply used as presented in the centrifuge study by McVay et al. [8] and numerical simulation by Zhang et al. [7]. Whereas, the results from LPILE were back-fitted since the coefficient of subgrade reaction η_h was back-calculated as 2714 kN/m^3 (Zhang et al. [7]).
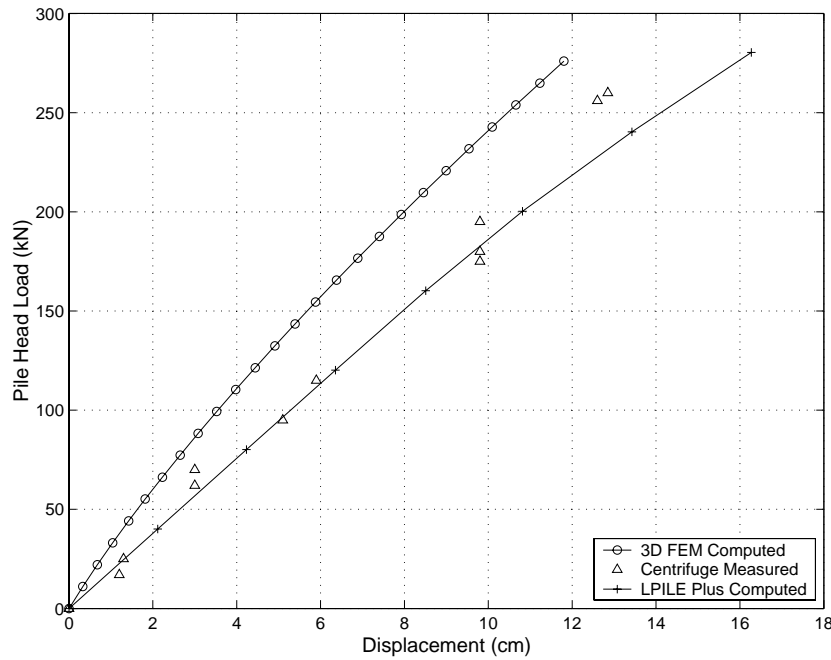

Figure 20. Simulated versus experimental pile head displacements.

The bending moments, shear forces and lateral pressures of uniform sand and clay profiles

from 3D FEM and LPILE were plotted against pile depth at several pile head loads in Figure 21 and 22. In general, there is a good agreement between the results from FEM and LPILE in uniform sand profile. In uniform soft clay profile, it is noted that the pressures at shallow depth from LPILE are smaller than those computed by FEM, which agrees with one of the findings by the work of Steven and Audibert [14]. For example, the pressures at lateral load of 120kN and 200kN from LPILE are only about half of those from FEM. Because the pressures at shallow depths are so small in LPILE that the pile head has to deform much more than in FEM and the passive pressure zone in LPILE extends to fairly large depth.

Since LPILE currently uses the equivalent depth method developed by Geogiadis [4] for layered soil profiles, the LPILE output pressure distribution along pile depth, especially across the layer interface does not take into account of the layering effect, thus it is not that meaningful to compare pressure distributions of layered profiles from LPILE versus FEM.

It is also interesting to compare the $p - y$ curves derived from FEM with those used in LPILE. Figures 24 and 23 show FEM derived and LPILE used $p - y$ curves for uniform clay and sand profiles, respectively. It should be noted that the coefficient of subgrade reaction η_h was again back-calculated as 8969 kN/m^3 in order to get a reasonable $p - y$ curves. From Figures 24 (a) and (b), it is clear that $p - y$ curves in sand profile from LPILE have lower resistance at depth close to ground surface. The $p - y$ curves for clay profile shown in Figures 24 (a) and (b) are seen to have much lower resistance at shallow depths.

4. SUMMARY

This paper presents results from a finite element study on the behavior of a single pile in elastic–plastic soils. The analysis included single pile behavior in sand, clay and layered soils.
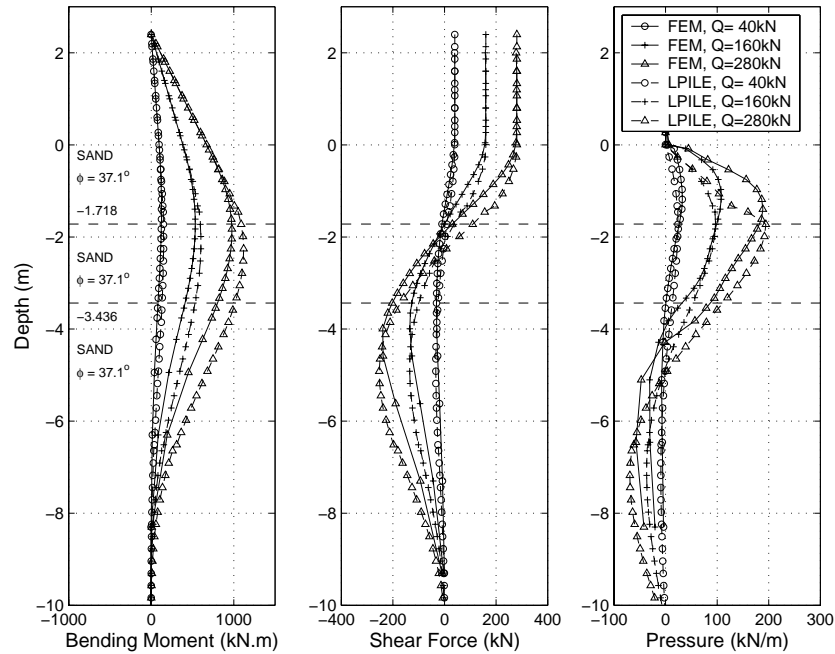
Figure 21. Comparison of bending moment, shear force and pressure computed by FEM and LPILE
in uniform sand profile(case #3).

Based on the results presented, it is concluded that three dimensional finite element analysis
using very simple elastic-plastic soil models can predict the pile head deflection with very good
accuracy.

The main findings of this numerical study can be summarized as follows:

- When a sand layer is present within a clay deposit, the increase in lateral pressure in clay
  near the interface is confined to a narrow zone, up to two times of pile width, therefore
  the layering effect in this case is not prominent.

- When a clay layer is present within a sand deposit, the reduction in pressures spread
  well into the sand layer (up to four times of pile width). The layering effects are of more
  importance in this case since the disturbance zone is large and the pressure reduction is
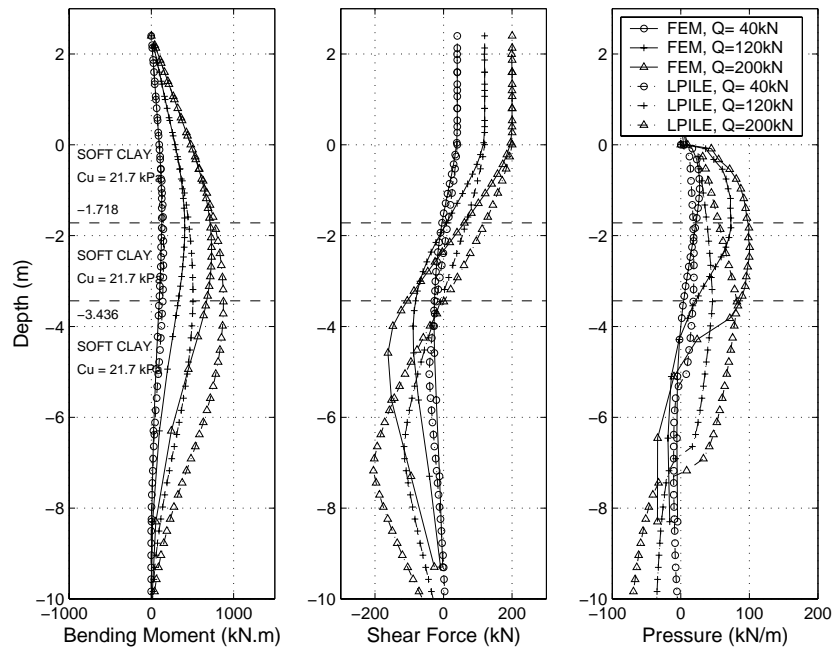
Figure 22. Comparison of bending moment, shear force and pressure computed by FEM and LPILE
in uniform soft clay profile(case #1).

significant. Reduction factors are given in terms of charts of pressure reduction versus the distance from the interface.

In addition, comparison with centrifuge data shows generally a good agreement between the bending moments, shear forces and lateral resistance. Moreover, a comparison with results from program LPILE, used in extensively in practice, show some discrepancies ultimate pressures in shallow soil layers.
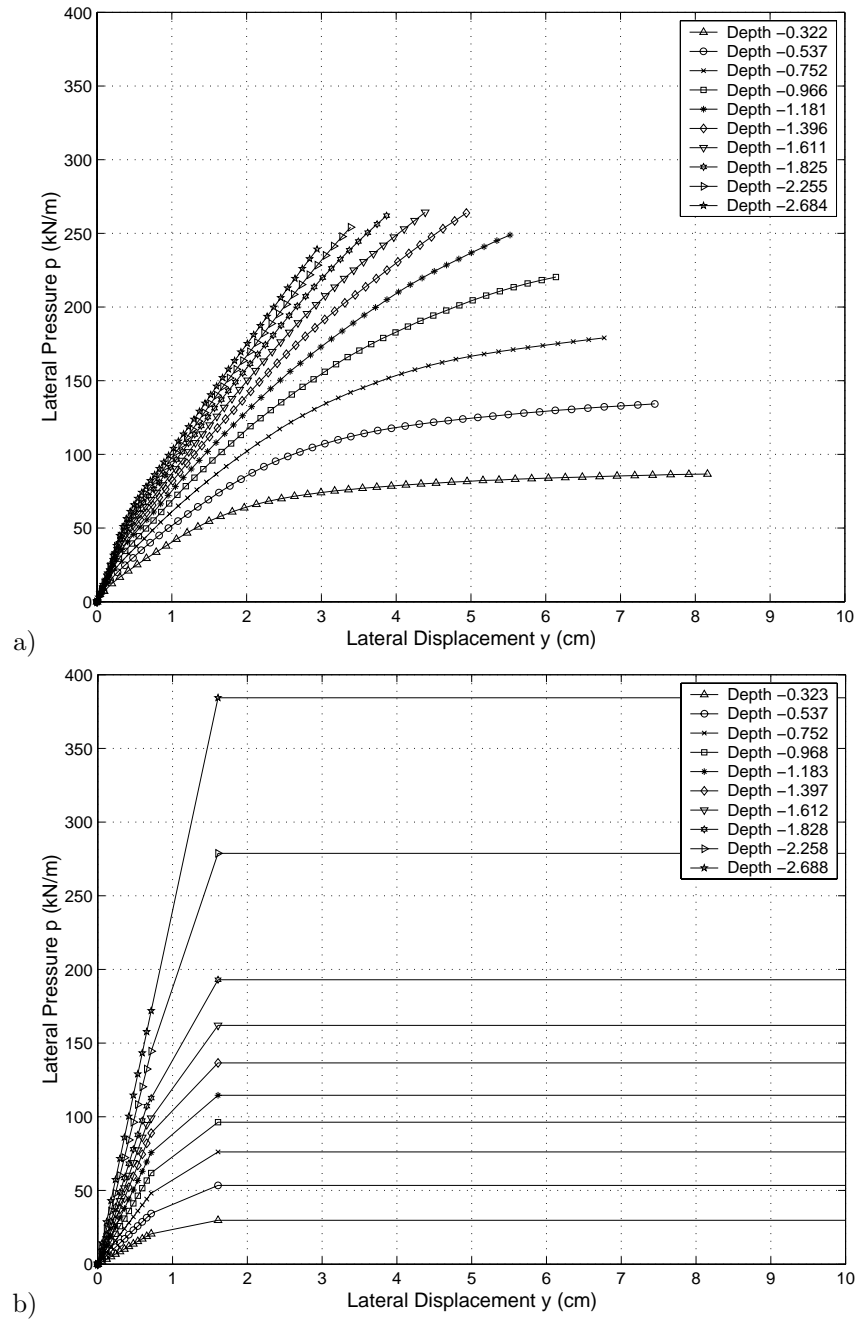
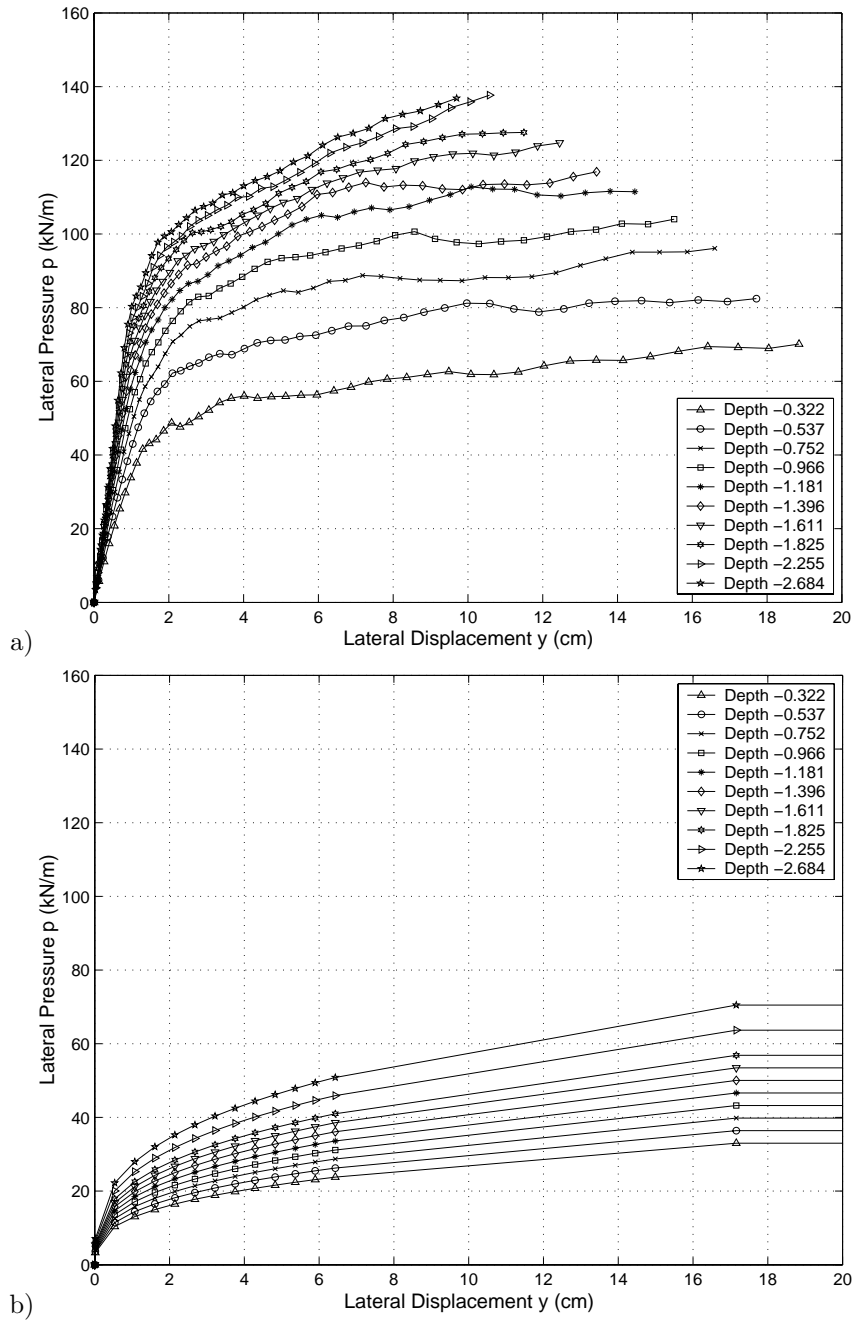Figure 23. $p - y$ curves from FEM (a) and LPILE (b) in uniform sand profile ($\eta_h = 8969 \ kN/m^3$, $\phi = 37.1^o$).

Figure 24. $p-y$ curves from FEM (a) and LPILE (b) in uniform clay profile ($\epsilon_{50} = 0.02$, $C_u = 21.6\ kPa$).

REFERENCES

1. Brown, D. A., and Shie, C.-F. Numerical experiments into group effects on the response of piles to lateral loading. *Computers and Geotechnics 10* (1990), 211–230.

2. Brown, D. A., and Shie, C.-F. Three dimensional finite element model of laterally loaded piles. *Computers and Geotechnics 10* (1990), 59–79.

3. Brown, D. A., and Shie, C.-F. Some numerical experiments with a three dimensional finite element model of a laterally loaded pile. *Computers and Geotechnics 12* (1991), 149–162.

4. Georgiadis, M. Development of p-y curves for layered soils. In *Geotechnical Practice in Offshore Engineering* (April 1983), Americal Society of Civil Engineers, pp. 536–545.

5. Jeremić, B., and Yang, Z. Template elastic–plastic computations in geomechanics. *International Journal for Numerical and Analytical Methods in Geomechanics* (November 2001). In print (December 2001), available as CGM report at: `http://sokocalo.engr.ucdavis.edu/~jeremic/publications/CGM0102.pdf`.

6. Kimura, M., Adachi, T., Kamei, H., and Zhang, F. 3-D finite element analyses of the ultimate behavior of laterally loaded cast-in-place concrete piles. In *Proceedings of the Fifth International Symposium on Numerical Models in Geomechanics, NUMOG V* (September 1995), G. N. Pande and S. Pietruszczak, Eds., A. A. Balkema, pp. 589–594.

7. Limin Zhang, M. M., and Lai, P. Numerical analysis of laterally loaded 3x3 to 7x3 pile groups in sands. *Journal of Geotechnical and Geoenvironmental Engineering 125*, 11 (Nov. 1999), 936–946.

8. McVay, M., Zhang, L., Molnit, T., and Lai, P. Centrifuge testing of large laterally loaded pile groups in sands. *Journal of Geotechnical and Geoenvironmental Engineering 124*, 10 (October 1998), 1016–1026.

9. Muqtadir, A., and Desai, C. S. Three dimensional analysis of a pile-group foundation. *International journal for numerical and analysis methods in geomechanics 10* (1986), 41–58.

10. OpenSees Development Team (Open Source Project). OpenSees: open system for earthquake engineering simulations.   , 1998-2002.

11. Pressley, J. S., and Poulos, H. G. Finite element analysis of mechanisms of pile group behavior. *International Journal for Numerical and Analytical Methods in Geomechanics 10* (1986), 213–221.

12. REESE, L. C., WANG, S. T., ISENHOWER, W. M., AND ARRELLAGA, J. A. *LPILE plus 4.0 Technical Manual*, version 4.0 ed. ENSOFT, INC., Oct. 2000.

13. REESE, L. C., WANG, S. T., M., I. W., A., A. J., AND J., H. *LPILE plus 4.0 User Guide*, version 4.0 ed. ENSOFT, INC., Oct. 2000.

14. STEVENS, J. B., AND AUDIBERT, J. M. E. Re-examination of p-y curve formulations. In *Eleventh Annual Offshore Technology Conference* (April 1979), vol. I, Americal Society of Civil Engineers, pp. 397–403.

15. TROCHANIS, A. M., BIELAK, J., AND CHRISTIANO, P. Three-dimensional nonlinear study of piles. *Journal of Geotechnical Engineering 117*, 3 (March 1991), 429–447.

16. WAKAI, A., GOSE, S., AND UGAI, K. 3-d elasto-plastic finite element analysis of pile foundations subjected to lateral loading. *Soil and Foundations 39*, 1 (Feb. 1999), 97–111.